

## Square plates as symmetrical anchor plates under uplift test in loose sand

Hamed Niroumand\* and Khairul Anuar Kassim<sup>a</sup>

*Department of Geotechnical Engineering, Faculty of Civil Engineering, Universiti Teknologi, Malaysia*

*(Received November 09, 2013, Revised January 25, 2014, Accepted February 06, 2014)*

**Abstract.** The uplift response of symmetrical square anchor plates has been evaluated in physical model tests and numerical simulations using Plaxis. The behavior of square anchor plates during uplift test was studied by experimental data and finite element analyses in loose sand. Validation of the analysis model was also carried out with 50 mm, 75 mm and 100 mm Length square plates in loose sand. Agreement between the uplift responses from the physical model tests and finite element modeling using PLAXIS 2D, based on 100 mm computed maximum displacements was excellent for square anchor plates. Numerical analysis using square anchor plates was conducted based on the hardening soil model (HSM). The research has shown that the finite element results are higher than the experimental findings in loose sand.

**Keywords:** uplift response; symmetrical anchor plate; square plate; loose sand; numerical modeling; plaxis; FEM; Hardening Soil Model (HSM)

---

### 1. Introduction

Many structural designs require foundation systems that can resist vertical or horizontal uplift loads. As part of a larger effort to improve the performance of foundation systems, guidelines have been developed for anchor system designs and installation. Various structures, such as transmission towers, tunnels, sea walls, buried pipelines, retaining walls, etc., are subjected to considerable uplift forces. In such cases, an absorbing and economic design solution may be obtained through the use of tension members. These elements, which are referred to as anchors, are generally fixed to the structure and embedded in the ground to an effective depth so that they can resist uplifting forces with safety.

Many researchers have investigated the influence of different parameters on the uplift response of horizontal anchors in sand. Many researchers, such as Mors (1959), Giffels *et al.* (1960), Balla (1961), Turner (1962), Ireland (1963), Sutherland (1965), Mariupolskii (1965), Kananyan (1966), Baker and Konder (1966), Adams and Hayes (1967), Andreadis *et al.* (1981), Dickin (1988), Fargic and Marovic (2003), Merfield and Sloan (2006), Dickin and Lama (2007), Kuzer and Kumar (2009), Kame *et al.* (2010, 2012), Adhami *et al.* (2012), and Bhattacharya and Kumar (2013a, b), were concerned with a general solution especially for an ultimate uplift capacity based on experimental works in sand, although Bhattacharya and Kumar (2013a, b) evaluated plate

---

\*Corresponding author, Post-Doc Researcher, E-mail: ham.niroumand@yahoo.com

<sup>a</sup> Ph.D.

anchors in clay. Also, many numerical studies have been reviewed on the behavior of symmetrical anchor plates since Meyerhof and Adams (1968) until the most recent analysis such as Kuzar and Kumar (2009). This analysis was pioneered by Vesic (1971), Sarac (1989), Smith (1989), Fargic and Marovic (2003), Merfield and Sloan (2006), Dickin and Laman (2007), and Kuzer and Kumar (2009). Increasing the use of symmetrical anchor plates to resist uplift response may be achieved by increasing the size and depth of an anchor or the improvement of soil in which these anchors are embedded, or both.

In summary, most of the existing works in the literature are mainly focused on the capacity of symmetrical anchor plates embedded in normal soils with a horizontal ground surface. However, a few researches have explored anchor plates embedded in different soil densities. However, to the knowledge of the authors, hardly any effort has been made so far to evaluate the performance of symmetrical square anchor plate located in different soil densities. Therefore, the effect of soil densities on stability and rupture surface of the soil and, hence, the symmetrical anchor plate capacity is unclear. The current research provides insight into the effect of loose sand on the response of horizontal square anchor plates that are embedded adjacent to a soil surface. The main objectives of the work are to study the loose sand in order to enhance the ultimate uplift response of symmetrical square anchor plates and determine the influence of embedment depth, soil density, failure mechanism and breakout factors.

## **2. Model tests**

### *2.1 Laboratory model tests*

### *2.2 Model box*

The cohesionless soil placement is particularly important during uplift tests. Similar cohesionless soil unit weights are obtained as a basis for comparing the influence of uplift parameters on the symmetrical anchor plate capacity. A sand unit weight at a value of  $14.99 \text{ kN/m}^3$  was decided for sand in loose packing, which was obtained using the cohesionless soil raining method. Trial tests were run in order to predict the particular conditions that had to exist before the target unit weight can be achieved. For cohesionless soil in loose condition, trial tests indicated that there was a limiting sand thickness before a significant change in sand unit weight across the sand thickness occurred. The standard cohesionless soil thickness was taken as 50 mm since this thickness gave a consistent value of unit weight when the cohesionless soil was rained from a certain height measured from the top of the cohesionless soil layer. Regarding the sand-raining test, a range of falling cohesionless soil heights were employed in order to obtain the height required for the desired unit weight. The influence of cohesionless soil thickness on the unit weight was also found to exist for cohesionless soil samples that had to be compacted in order to achieve the desired unit weight.

Uplift tests were carried out in two test boxes covering two areas. The first test box was used for failure tests and covered an area of  $600 \text{ mm} \times 250 \text{ mm}$  and 450 mm deep with side glass walls to enable observation of the movement and behavior of cohesionless soil. The second test box was used for uplift tests and covered an area of  $1000 \text{ mm} \times 500 \text{ mm}$  and 1200 mm deep. Fig. 1 shows the first box for the failure test. The loading frames were designed to suit the requirements of the tests.



Fig. 1 First test box for failure test

### 2.3 Test materials

Several tests were done to determine the properties of sand samples during experimental work. The tests included were:

- (1) Particle size distribution using dry sieve method (BS 1377: Part 2: 1990)
- (2) Maximum and minimum unit weight using vibratory table method (ASTM standards on soil compaction, 1993 edition, Test designation D4254-91 and D4253-93)
- (3) Direct shear test using small shear box (BS 1377: Part 7: 1990)
- (4) Particle density using small pycnometer method (BS 1377: Part 2: 1990)

### 2.4 Particle size distribution

The particle size distribution test was done according to BS 1377: Part 2:1990 using the dry sieve method. This method covers the quantitative determination of the particle size distribution in a cohesionless soil down to fine-sand dimensions. For each sand type, three dry sieve tests were done with sieve aperture sizes as follows; 2.36 mm, 1.18 mm, 0.6 mm, 0.3 mm, 0.212 mm, 0.15 mm and 0.075 mm.

The sieve sizes used were considered adequate to cover the range of the sand type used for the experimental work. The sand sample was passed through a series of standard test sieves and progressed through successional smaller size sieves. The weight of sand retained in each sieve is determined and the cumulative percentage by weight passing each sieve is calculated. Particle size distribution for sand type is presented as a curve on a semi-logarithmic plot, the ordinates being the percentage by weight of the particles smaller than the size given by the abscissa. The particle size distribution is shown below in Fig. 2.

Sand with particle sizes ranging from 0.2 to 0.6 mm is defined as medium sand whereas particle sizes of 0.6 to 2 mm are considered as coarse sand. The soils used were therefore classified as uniform medium sand with  $D_{50} = 0.50$  mm. The sand properties from particle size distribution analysis are summarized in Table 1.

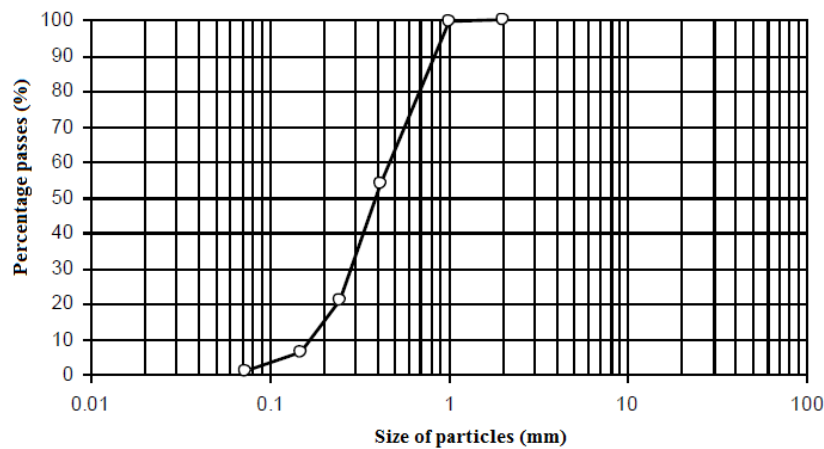


Fig. 2 Particle size distributions for sand sample

| Sand |        |        | Gravel |        |
|------|--------|--------|--------|--------|
| Fine | Medium | Course | Fine   | Course |

Table 1 Particle size properties of sand sample

| Particle size properties of sand analysis |                    |
|---|--------------------|
|   | Particle size (mm) |
| $D_{10}$                                  | 0.17               |
| $D_{30}$                                  | 0.32               |
| $D_{60}$                                  | 0.55               |
| $C_u$                                     | 2.8                |
| $C_c$                                     | 1                  |
| Percent of middle sand                    | 45.7%              |
| Percent of fine sand                      | 54.3%              |
| Percentage of coarse sand                 | 0%                 |

### 2.5 Minimum sand unit weight

The minimum unit weight represents the loosest condition of a sand free draining soil that can be attained by laboratory procedure. The procedure essentially prevents bulking and minimizes particle segregation. In general, this particular procedure consists of determining the unit weight of oven-dried soil placed into a container of known volume in such a manner that it minimizes compaction of the soil.

The maximum unit weight of a given free draining soil is determined by placing an oven dried soil in a mold, and applying a dead weight to the surface of the soil. The mold, soil and dead weight are then vibrated vertically using an electromagnetic vibrating table for a certain period. The maximum unit weight is obtained by dividing the oven dried soil mass by its volume.

The relative unit weight expresses the degree of compactness of a cohesionless soil with respect to the loosest and densest condition as defined by laboratory steps.

Only when viewed against the possible range of variation, in terms of the relative unit weight, can the dry unit weight be related to the compaction effort used to place the soil in a compacted fill and the stress- strain tendencies of the soil when subjected to external loading. It is therefore generally recognized that the relative unit weight is a good indicator of the state of compactness of a given soil mass.

The maximum and minimum unit weights for the sand samples were obtained through tests with designation D4254-91 as recommended in ASTM standards on soil compaction (1993). ASTM standards on soil compaction (1993) with designation D4254-91 recommends the standard soil test method for obtaining the minimum index density/unit weight and calculation of relative density. Three alternative procedures were suggested to determine the minimum index density/unit weight, as follows:

- (1) Test method A – using a funnel pouring device or a hand scoop to deposit the material in the mold,
- (2) Test method B – depositing material into a mold by extracting a soil filled tube,
- (3) Test method C – depositing material by inverting a graduated cylinder.

Test method A is the preferred procedure to be used in conjunction with ASTM standards on soil compaction (1993) designation D4253 whereas Test Methods B and C are for testing used in conjunction with special studies.

ASTM standards on soil compaction (1993) test designation D4253 provide the recommended standard test methods for obtaining maximum index density and unit weight using a vibratory table. Four alternative procedures are suggested to determine the maximum index density and unit weight:

- (1) Test method 1A – using oven dried soil and an electromagnetic vertically vibrating table.
- (2) Test method 1B – using wet soil and an electromagnetic vertically vibrating table.
- (3) Test method 2A – using oven dried soil and an eccentric or cam-driven vertically vibrating table.
- (4) Test method 2B – using wet soil and an eccentric or cam-driven vertically vibrating table.

For the purpose of this study, Test method 1A was used based upon available equipment. The results of the maximum and minimum unit weights are presented below in Table 2 for sand samples.

### 2.6 Direct shear test using small shear box

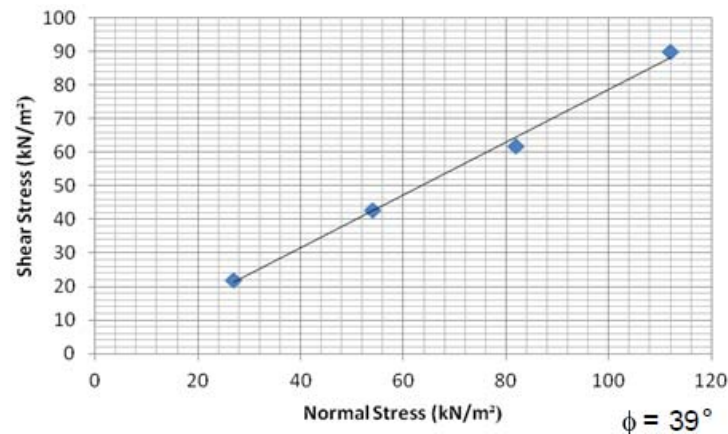
The direct shear test includes the testing of a square prism of soil that is laterally restrained and sheared along a mechanically involved horizontal plane while subjected to a pressure applied normal to the shearing plane. The shearing resistance is measured at regular intervals using at

Table 2 Results of standard test methods for minimum unit weights of sand using a vibratory table

| Uniform sand  | First sample | Second sample | Third sample | Average unit weight |
|---|--------------|---------------|--------------|---------------------|
| Minimum unit weight, $\gamma_{\min}$ (kN/m <sup>3</sup> ) | 15.04        | 14.91         | 15.02        | 14.99               |

Table 3 Normal stress acting on sand sample during direct shear test

|                                    | 1 <sup>st</sup> sample | 2nd sample | 3 <sup>rd</sup> sample | 4 <sup>th</sup> sample |
|------------------------------------|------------------------|------------|------------------------|------------------------|
| Normal stress (kN/m <sup>2</sup> ) | 27                     | 54         | 82                     | 112                    |

Fig. 3 Variation of shear stress  $\tau$ , versus normal stress  $\sigma$  for direct shear tests

datalogger and tests were carried out with four samples using different normal pressures until the shearing resistance reached a maximum value for which the soil can sustain. The relationship between measured shear stress failure and stress applied normal to the plane enables deriving the effective shear strength parameters  $c$  and internal friction  $\phi$ .

The normal stress acting on uniform sand in the direct shear test conducted for this research is given in Table 3.

Results of the direct shear tests conducted on uniform sand are given in Fig. 3. Derivation of the internal friction  $\phi$  is obtained from the slope variation of the shear stress  $\tau$  with the normal stress  $\sigma$ .

A summary of the sand properties and results for the direct shear tests are presented in Table 4.

### 2.7 Particle density using small Pyknometer Method

The term 'particle density' is used instead of the term 'specific gravity' in the updated version of this particular standard (BS 1377, Part 2: 1990). There are basically three procedures subscribed, namely:

- (1) Gas jar method: suitable for most soils involving those containing gravel-sized particles.
- (2) Small pyknometer method: the more definitive method for soils consisting of clay, silt and sand-sized particles.
- (3) Pyknometer method: suitable for most soils up to medium gravel size and the least accurate compared to the previous two methods.

The test for particle density was conducted using the small pyknometer method for the purpose of this research as the facilities were readily available and the method is suitable. Tests were done

Table 4 Summary of soil properties and results of  $\phi$  from direct shear tests (BS 1377, Part7: 1990)

|  | Loose sand |
|--|------------|
| Unit weight ( $\text{kN/m}^3$ )                | 14.99      |
| $\phi$ ( $^\circ$ ) in plane strain condition  | 39         |
| $\phi$ ( $^\circ$ ) in 3-dimensional condition | 38         |

Table 5 Summary of particle density test on uniform sand

| Bottle No.  | 1 <sup>st</sup> sample | 2 <sup>nd</sup> sample | 3 <sup>rd</sup> sample |
|---|------------------------|------------------------|------------------------|
| Mass of bottle ( $w_1$ ) gm   | 27.30                  | 30.45                  | 29.70                  |
| Mass of bottle+ sand ( $w_2$ ) gm   | 34.75                  | 39.10                  | 38.64                  |
| Mass of bottle + sand + water ( $w_3$ ) gm  | 82.35                  | 86.45                  | 85.30                  |
| Mass of bottle + water ( $w_4$ ) gm   | 77.64                  | 81.50                  | 79.80                  |
| Mass of sand ( $w_2-w_1$ ) gm   | 7.49                   | 8.63                   | 8.96                   |
| Mass of water whose volume is equivalent to sand ( $w_4-w_1$ )-(w <sub>3</sub> -w <sub>2</sub> ) gm | 2.78                   | 3.70                   | 3.46                   |
| Particle density of sand $\rho_s = \frac{w_2 - w_1}{(w_4 - w_1) - (w_3 - w_2)}$                     | 2.64                   | 2.63                   | 2.64                   |
| Average particle density, $\rho_s$  |                        | 2.64                   |                        |

Table 6 Summary of soil properties for tests previously undertaken

| Conditions | Uniform sand                           |
|------------|--|
|            | $\phi = 38^\circ$                      |
|            | $G_s = 2.64$                           |
| Loose      | $\gamma_{\min} = 14.99 \text{ kN/m}^3$ |



Fig. 4 Symmetrical square anchor plates

on three samples for sand and the average value for particle density is used. Results of the test can be found in Table 5.

### *2.8 Summary of Soil Properties*

A summary of soil properties for all tests conducted, as described beforehand, is given in Table 6.

### *2.9 Model symmetrical anchor plate*

The uplift tests of symmetrical anchor plate geometry of the model square plates that were used anchorage. Model anchors with 10 mm thick rigid plates are obtained. Experiments 5.0, 7.5 and 10 cm diameter circular plates has been used, including different anchor plates as illustrated in Fig. 4.

### *2.10 Experimental test*

The uplift test was conducted in the geotechnical laboratory. The main treatment to be observed during the experimental test was the stress-displacement relationship during symmetrical anchor plate breakout. The set up of the uplift test steps are described in the following sections.

A schematic experimental set up is shown in Fig. 5. The test boxes were used to contain cohesionless soil as embedment pattern. The model symmetrical anchor plates are connected to a pulling tendon cable for uplifting. A quasi static rate of pullout of approximately 1.5 mm/min was used for every test. This is to ensure that the symmetrical anchor plates surrounding element will have ample time to redistribute during uplift. Uplift capacity was measured by load cell attached to the pulling tendon cable during the uplift test. A linear variable displacement transducer (LVDT) was placed at the top of the symmetrical anchor plate holder to measure the vertical displacement so as to predict the amount of symmetrical anchor plate movement required to mobilize the ultimate uplift capacity. A motor was connected to the pulling tendon cable via tendon steel cables. Datalogger was used to record data readout from the load cell and LVDT.



Fig. 5 The setup of the uplift test

### 2.11 Uplift test procedure

The uplift test takes into account only the net uplift capacity of the symmetrical anchor plates. This would mean that only the symmetrical anchor plates are involved in the analysis of their uplift capacity. The test procedure for model symmetrical anchor plates tested in uplift included the following steps:

- (1) Symmetrical anchor plate models to be tested are attached accordingly to the tendon cable, which is then connected to the load cell holder. All apparatus included in the test are controlled for default before movement of symmetrical anchor plates in the test boxes. These controls include;
  - (a) Inspection of test frame to ensure rigidity,
  - (b) Inspection of pulling tendon cable to ensure that it has not worn out,
  - (c) Ensuring that the test boxes are empty and free of cohesionless soil particles,
  - (d) Ensuring that the tendon cable connected to the load cell holder is firmly in place.
- (2) The symmetrical anchor plate model to be tested is lowered slowly into the test box to the intended depth marked before hand to ensure that vertical pullout is axially loaded. The symmetrical anchor plate is controlled again for verticality using the spirit level.
- (3) The cohesionless soil is then placed in the box according to the placement method described previously.
- (4) After the required height is reached, the surface layer is then flushed and the load cell and LVDT are then placed into position.
- (5) Calibration of the load cell and the LVDT were done earlier, so that only the net uplift response and the vertical displacement measurements must be fed to the datalogger.
- (6) The datalogger is then initiated and readings at predefined intervals are recorded.
- (7) The symmetrical anchor plate is considered to have undergone failure when a peak uplift response value is deemed to have been reached.
- (8) The cohesionless soil used for testing is then weighted and calculated for its unit weight.

The test must be repeated if the desired unit weight was not achieved. Also if disturbance to any part of the experimental set up occurred during testing, such as human error and power shortage that may have caused discontinuity of the test being conducted. All factors should indicate that the data obtained from the test was reliable before the data is accepted for analysis.

The test procedure undergone in this paper was considered adequate to cover the range of parameters under study and to systematically isolate the effects of a certain parameter on the uplift capacity. This enabled a critical analysis of the experiments and numerical simulations conducted and provided a basis for comparison.

### 2.12 Failure mechanism

The failure mechanism tests were performed in Fig. 6. In these tests, patterns were made on the extreme uplift loads and embedment ratio. The aim of these tests was to show the behavior of failure mechanisms of loose and dense sand around symmetrical anchor plates under uplift forces.

The properties of the test were applied per unit weight of  $14.99 \text{ kN/m}^3$  to obtain loose sand. Every 50 mm vertical interval had a 4 mm dyed strip of sand that was placed on the front face of the failure box for easy viewing. Loading was applied to the square anchor plates with a loading cable at a constant low rate in loose sand. The failure pattern was shown during the testing. The



Fig. 6 Set up of failure mechanism

symmetrical anchor plates were made to move until a sufficient distance was achieved, to ensure that the failure pattern was apparent.

### 2.13 Breakout factor

The main parameters of a collapse load acting on soil parameters are unit weight of sand, internal friction, symmetrical anchor plate's embedded depth and the size of symmetrical anchor plates. In a full scale model analysis, the equation of those parameters may be expressed in dimensionless quantities as

$$f_1(P, L, D, \emptyset, \gamma) = 0 \quad (3)$$

$f_1$  may be expressed as  $f_2$ , where

$$f_2(\pi_1, \pi_2, \pi_3) = 0 \quad (4)$$

Since the  $\emptyset$  is a dimensionless unit, thus

$$\pi_1 = \emptyset \quad (5)$$

Then

$$P = f(L, D, \gamma)$$

$$P = L^\alpha D^\beta \gamma^c$$

$$MLT^{-2} = (L)^\alpha (L)^\beta (ML^{-2}T^{-2})^c$$

$$\alpha = 1, \beta = 2, c = 1$$

Then

$$\begin{aligned} P &= LD^2\gamma \\ \pi_2 &= P/LD^2\gamma \end{aligned} \quad (6)$$

$L$  and  $D$  have the same dimensional form, so

$$\pi_3 = L/D \quad (7)$$

Thus

$$f_1(\emptyset, P/LD^2\gamma, L/D) = 0 \quad (8)$$

$$\frac{P}{LD^2\gamma} = f\left(\emptyset, \frac{L}{D}\right) \quad (9)$$

$$P = f\left(\emptyset, \frac{L}{D}\right) \times LD^2\lambda$$

Where  $P$  is the ultimate uplift load obtained from the test,  $D$  is the width of the anchor plate,  $H$  is the embedded depth of the anchor plate,  $\gamma$  is the dry unit weight,  $\emptyset$  is the internal friction angle and  $L/D$  is the embedment ratio. Internal friction angle is constraint for the test.

### 3. Numerical simulation models

A series of two-dimensional finite element analyses (FEA) on a prototype symmetrical anchor plate - sand system was performed in order to assess the experimental model test results and find out the deformations behavior within the sand body. The analysis was performed under the finite element program, Plaxis package (professional version 8, Bringgreve and Vermeer 1998). Plaxis is geotechnical software that can analyze soil problems. In general, the initial conditions comprise the initial groundwater conditions, the initial geometry configuration and the initial effective stress state. The sand layer in this research was dry, so there was no need to enter ground water conditions. The analysis was done by means of Hardening Soil Model (HSM). The geometry of the prototype anchor plate-box system was supposed to be the same as the experimental model. The same gradient, steel plate for the symmetrical anchor plate and the same sand that were used in the model test were also used in the prototype research. Tables 7 and 8 illustrate the sand, geogrid and plate properties used.

A variety of sand models were made in the computer code chosen for this research. The Hardening Soil Model (HSM) criteria was used to model the sand on account of its analysis, practical importance and the availability of the parameters needed. The interaction between the symmetrical anchor plates, geogrid and sand was modeled by means of interface elements, which enabled specifying a reduced wall friction compared to the soil friction. The parameters used for numerical simulation are depicted in Tables 7 and 8. The model geometry, based on the finite element method by means of Plaxis and verified for the analysis, is shown in Fig. 7. The left vertical line of the geometry model was constrained horizontally, but the bottom horizontal boundary was constrained in both the horizontal and vertical directions. The prescribed load was loaded on in increments, accompanied with iterative analysis up to failure. The boundary conditions presented permit the vertical boundary to be free vertically and constrained horizontally until the bottom horizontal boundary is completely fixed. The program can be the automatic

Table 7 Material properties used in Plaxis

| Parameter value  | Loose packing |
|--|---------------|
| Cohesion, $c$ (kPa)  | 0.5           |
| Residual angle of internal friction ( $^{\circ}$ )           | 38            |
| Angle of dilatancy ( $\Psi^{\circ}$ )                        | 8             |
| Unit weight, $\gamma$ (kN/m <sup>3</sup> )                   | 14.99         |
| Secant stiffness, $E_{50}$ (kN/m <sup>2</sup> )              | 20000         |
| Initial stiffness, $E_{OED}$ (kN/m <sup>2</sup> )            | 20000         |
| Unloading/reloading stiffness, $E_{UR}$ (kN/m <sup>2</sup> ) | 60000         |
| Poisson's ratio  | 0.2           |
| Power for stiffness stress dependency, (m)                   | 0.5           |
| At rest earth pressure coefficient, $K_0$                    | 0.38          |
| $R_{inter}$  | 0.9           |

Table 8 Steel Plate Properties

| Type | Steel plates            |
|------|-------------------------|
| EI   | 163 kNm <sup>2</sup> /m |
| EA   | $3.4 \times 10^5$ kN/m  |

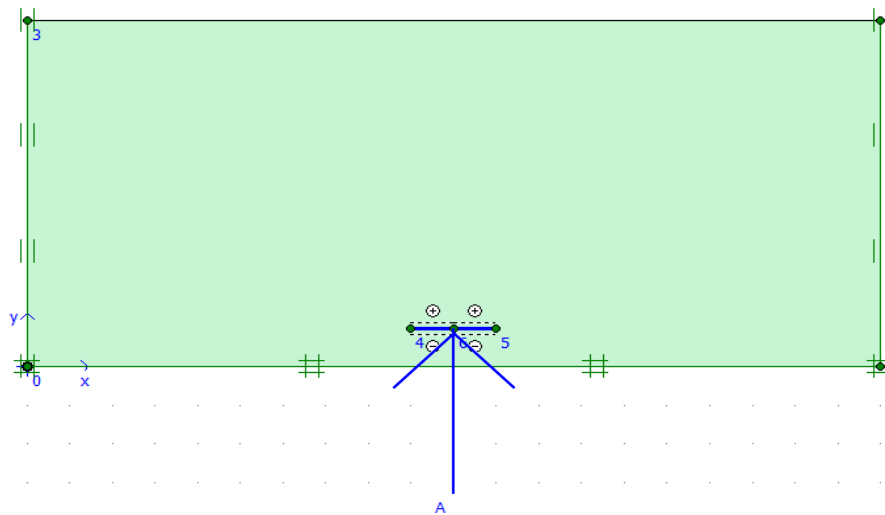


Fig. 7 The model geometry on prototype in Plaxis

produce of six node triangle plane strain elements for the sand and three node tensile elements for the symmetrical anchor plate. The analyzed geometry and produced mesh and related boundary conditions are shown in Fig. 7.

Table 9 Summary of uplift capacity result ( $L/D = 4$ )

| Symmetrical anchor plate<br>Types | Uplift capacity in loose sand ( $N$ ) |        |
|-----------------------------------|---------------------------------------|--------|
|                                   | Lab                                   | Plaxis |
|                                   | Loose sand                            |        |
|                                   | Square                                |        |
| Diameter = 5 cm                   | 152                                   | 186    |
| Diameter = 7.5 cm                 | 342                                   | 420    |
| Diameter = 10 cm                  | 640                                   | 780    |

### 4. Results

This part presents the results of the uplift experiments and models conducted for the uplift test. The uplift force-displacement relationship of symmetrical anchor plates when subjected to uplift were recorded and subsequently analyzed based on the peak uplift resistance of every particular test and simulation model determined by the finite element method using PLAXIS. The discussion involves the numerical and experimental aspects of net symmetrical anchor plate capacity during uplift test and symmetrical anchor plate displacement in loose sand. A rational basis for the behavior of symmetrical anchor plates studied in soil failure mechanism studies is conducted to obtain evidence on the shape and extent of soil shape failure when subjected to varying parameters. Sand was used as an embedment medium in this research. A loose packing was achieved by sand raining methods.

The effect of embedment ratio, breakout factor, and failure mechanism patterns of models were detailed on loose sand in numerical and experimental tests. The results were collected and

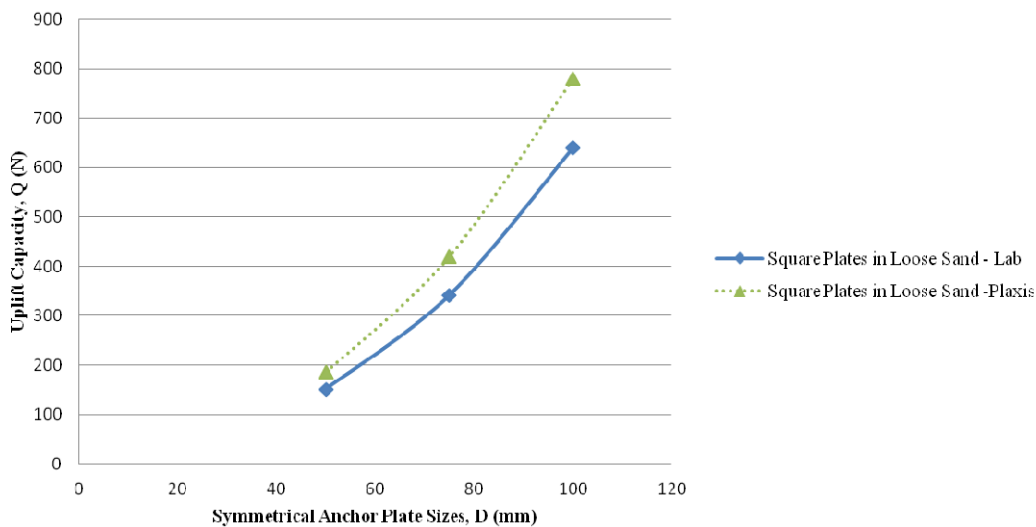


Fig. 8 Variation in uplift capacity  $Q$  with square symmetrical anchor plate size  $D$

presented in many graphs. The failure mechanism patterns of models in loose sand and dense sand were observed based on experimental and numerical analysis in this part. A summary of uplift test results is presented in Table 9 for symmetrical square anchor plates based on loose sand in the simulation and experimental work.

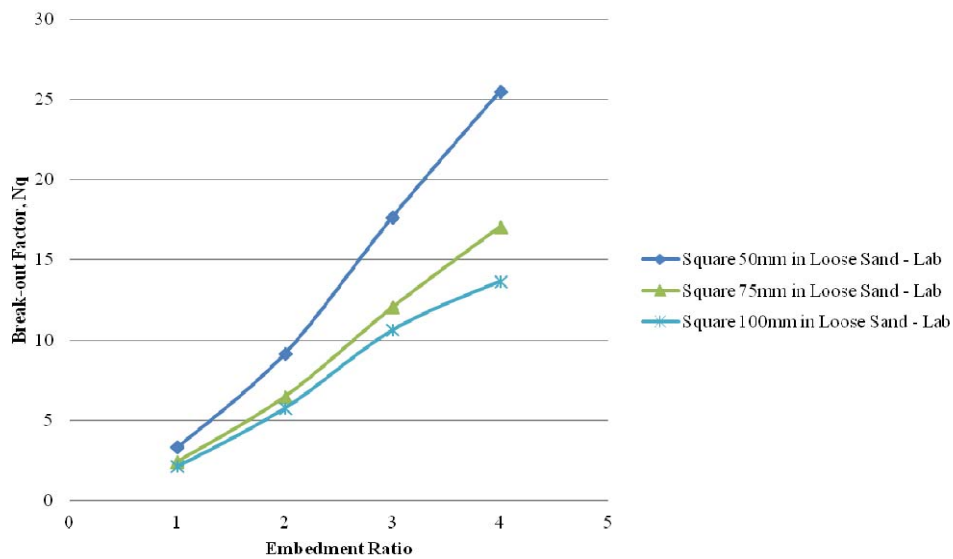


Fig. 9 Variation of breakout factor  $Nq$  with embedment ratio  $L/D$  for symmetrical square anchor plates in both loose conditions in laboratory

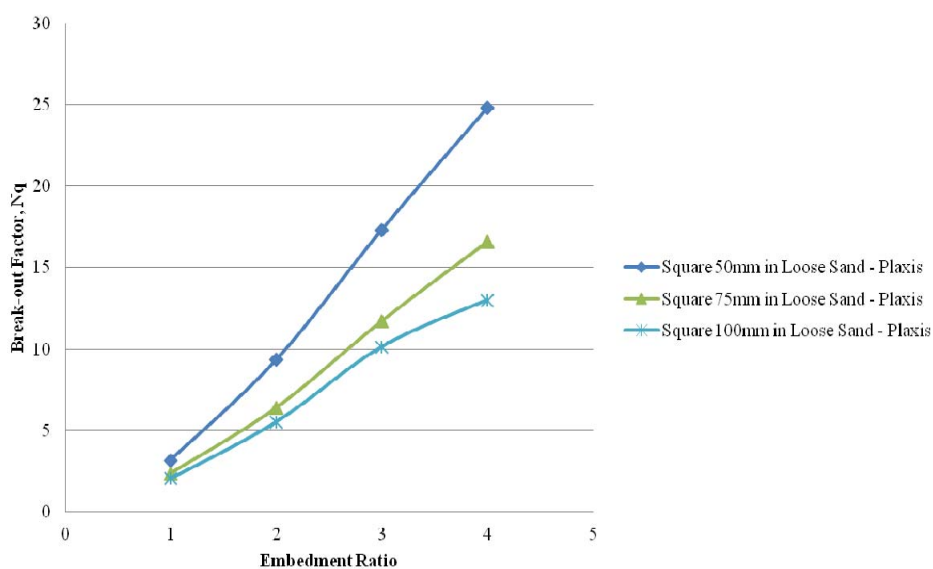


Fig. 10 Variation of breakout factor  $Nq$  with embedment ratio  $L/D$  for symmetrical square anchor plates in both loose conditions in Plaxis

The discussion of uplift capacity dealt with the parameters of the symmetrical anchor plate's sizes, sand packing and embedment ratio separately. This was to enable an impartial and focused review of the effects of each parameter on the symmetrical anchor plate during uplift in loose sand.

With reference to Fig. 8, symmetrical anchor plates experienced an increase in uplift capacity for every increase of the symmetrical square anchor plate's size. From Figure 8 shown below, the significant trend to note is a decrease in the rate of percentage increase in uplift capacity with an increase in the symmetrical anchor plate's size for the tests conducted. This is related to the trend of the percentage increase in symmetrical anchor plate's size with increasing depth, discussed in previous sections.

With regard to Fig. 9, symmetrical anchor plates experienced an increase in uplift capacity for every increase of embedment ratio in symmetrical anchor plate. As seen in Fig. 10, symmetrical anchor plates in maximum embedment ratio,  $L/D=4$ , had higher uplift capacities than symmetrical anchor plates in minimum embedment ratio  $L/D = 1$ .

#### 4.1 Failure mechanism studies

Studies on uplift failure mechanisms have shown that symmetrical anchor plates fail with a curved shear surface. An example of this is shown in Figs. 11 to 12. The figures illustrate the shear failure mechanism during uplift for symmetrical anchor plates in loose sand. The condition of sand surrounding the symmetrical square anchor plates before uplift is illustrated in Fig. 11. At the actual moment when the uplift capacity was reached, as illustrated in Fig. 12, the deformation experienced by the sand indicated a proponent failure surface. A certain degree of collapse occurred near the symmetrical square anchor plates. With further uplift movement, the failure surface was seen to be defined more prominently. The final failure surface is seen much clearer in Fig. 12, where a curved shaped localized failure occurred when the symmetrical anchor plate was pulled out at a constant rate. A contributing factor towards the formation of the curved shaped failure would be the collapse of soil around the symmetrical anchor plate to fill in the void formed near the symmetrical anchor plate's bottom.



Fig. 11 Initial state of sand before commencement of uplift in loose sand

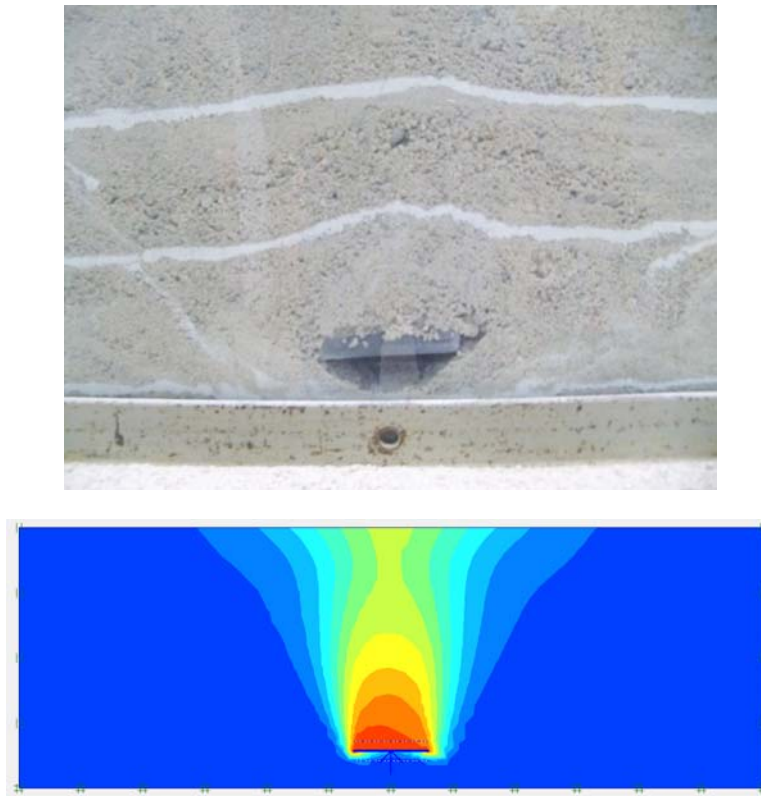


Fig. 12 State of sand after commencement of uplift in loose sand

## 5. Discussion

This part presents a comparison of theoretical and experimental values for the experimental and numerical program conducted. The literature review has explained previous theoretical research results, which were dedicated to the limiting ultimate uplift capacity of symmetrical anchor plates, their breakout factor and failure zones. Researchers such as Balla (1961), Meyerhof and Adams (1968), Vesic (1971), Rowe and Davis (1982), Murray and Geddes (1987), Sarac (1989), Smith (1989), Fargic and Marovic (2003), Merfield and Sloan (2006), Dickin and Laman (2007), Kuzer and Kumar (2009) and Niroumand *et al.* (2011) determined their parametric relationship for ultimate uplift capacity of anchor plates and their breakout factor.

Researchers such as Balla (1961), Meyerhof and Adams (1968), Vesic (1971), Rowe and Davis (1982), Murray and Geddes (1987), dedicated their works in proposing the theories of horizontal anchor plates subjected to uplift loads. This part presents a comparison of existing theories for the current research conducted. Fig. 13 illustrates a comparison of theoretical and experimental values as forwarded by various researchers such as Balla (1961), Meyerhof and Adams (1968), Vesic (1971), Rowe and Davis (1982), Murray and Geddes (1987) and the current research. The difference between each theoretical prediction lies in the value of the breakout factor in uplift and

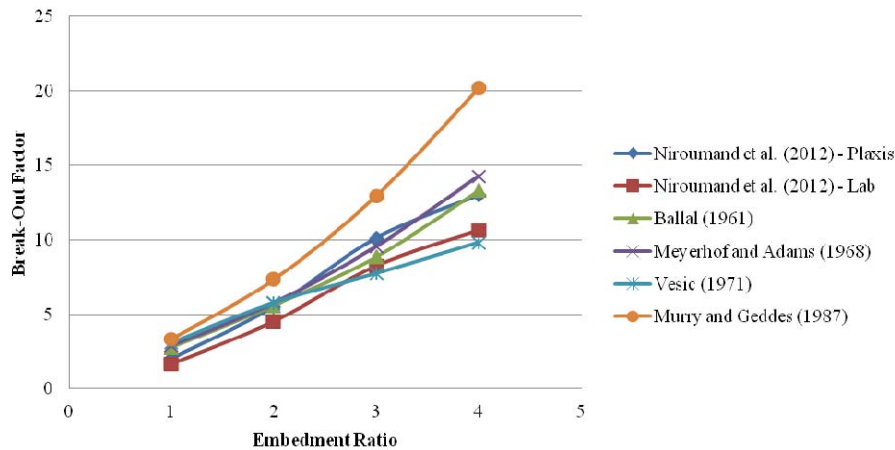


Fig. 13 Comparison of breakout factor between experimental results and theoretical and numerical prediction for square anchor plates in loose packing

other parameters. Balla (1961), Meyerhof and Adams (1968), Vesic (1971), Rowe and Davis (1982), Murray and Geddes (1987) proposed theoretical values based on the curved failure model by using the analytical and experimental evaluation method in loose sand. Fig. 13 illustrates comparison of theoretical breakout factor values and current results based on experimental and numerical analysis. The overall trend indicates that for the series of tests and models conducted, experimental and numerical values are in close agreement and similar to values of Balla (1961) for square plates.

## 6. Conclusions

A parametric research was conducted to obtain knowledge on symmetrical anchor plates, soil conditions and behavior of the symmetrical anchor plates during uplift. Although it is not dedicated to any specific practical conditions in engineering practice, it is useful to study its various affecting factors that influence the symmetrical anchor plate's capacity when subjected to uplift forces. The failure shape for symmetrical anchor plates with embedment ratio  $L/D$  up to 4 is cylindrical, despite variation in size and sand density when subjected to uplift loads.

In the selection of the symmetrical anchor plate's depth to achieve an economic anchor plate uplift design, the size and depth are important parameters to be taken into consideration. It would therefore be more economical and rational to increase the uplift capacity of symmetrical anchor plates by increasing their depth. This would help to significantly increase their uplift capacity more than simply increasing their size and thus their contact area with the sand.

## Acknowledgments

This research was partially supported by the research Grant at UTM, Malaysia (GUP Grant), and the project name is "uplift response of symmetrical anchor plates in grid fixed reinforced in

cohesionless soil”.

## References

- Adams, J.I. and Hayes, D.C. (1967), “The uplift capacity of shallow foundations”, *Ontario Hydro-Research Quarterly*, **19**(1), 1-15.
- Adhami, B., Niroumand, H. and Khanlari, K. (2012), “A new algorithm for the system identification of shear structures”, *Adv. Mater Res.*, **457-458**, 495-499.
- Andreadis, A., Harvey, R.C. and Burley, E. (1981), “Embedded anchor response to uplift loading”, *J. Geotech. Engrg. Div.*, **107**(1), 59-78.
- Baker, W.H. and Kondner, R.L. (1966), “Pullout load capacity of a circular earth anchor buried in sand”, *Highway Res. Rec.*, **108**, 1-10.
- Balla, A. (1961), “The resistance of breaking-out of mushroom foundations for pylons”, *Proceedings of the 5th International Conference Soil Mechanics and Foundation Engineering*, Paris, France, July, Vol. 1, pp. 569-576.
- Bhattacharya, P. and Kumar, J. (2012), “Horizontal pullout capacity of a group of two vertical strip anchors plates embedded in sand”, *Geotech. Geol. Eng.*, **3**(2), 513-521.
- Bhattacharya, P. and Kumar, J. (2013a), “Horizontal pullout capacity of a group of two vertical plate anchors in clay”, *Geomech. Eng., Int. J.*, **5**(4), 299-312.
- Bhattacharya, P. and Kumar, J. (2013b), “Seismic pullout capacity of vertical anchors in sand”, *Geomech. Geoeng.*, **8**(3), 191-201.
- Bildik, S. (2010), “An investigation of uplift resistance in foundation engineering and the analysis of uplift resistance of different type of foundations”, Master Thesis, Çukurova University, Turkey.
- Bowling, T. (2012), “Simplified analysis of the strength of anchor plates in a cohesionless soil: Part 2 – Experimental corroboration”, *Australian Geomech. J.*, **47**(2), 11-16.
- Bringgreve, R. and Vermeer, P. (1998), *PLAXIS-Finite Element Code for Soil and Rock Analysis*, Version 7, Plaxis BV, The Netherlands.
- Chattopadhyay, B.C. and Pise, P.J. (1986), “Breakout resistance of horizontal anchors in sand”, *Soil. Found.*, **26**(4), 16-22.
- Das, B.M. and Seeley, G.R. (1975a), “Inclined load resistance of anchors in sand”, *J. Geotech. Engrg. Div.*, **101**(GT9), 995-1008.
- Das, B.M. and Seeley, G.R. (1975b), “Breakout resistance of shallow horizontal anchors”, *J. Geotech. Engrg. Div.*, **101**(9), 999-1003.
- Dickin, E.A. (1988), “Uplift behavior of horizontal anchor plates in sand”, *J. Geotech. Engrg. Div.*, **114**(11), 1300-1317.
- Dickin, E.A. and Leung, C.F. (1992), “The influence of foundation geometry on the uplift behavior of piles with enlarged bases in sand”, *Can. Geotech. J.*, **29**(3), 498-505.
- Dickin, E.A. and Laman, M. (2007), “Uplift response of strip anchors in cohesionless soil”, *J. Adv. Eng. Softwares*, **38**(8-9), 618-625.
- Frgic, L. and Marovic, P. (2003), “Pullout capacity of spatial anchors”, *J. Eng. Comput.*, **21**(6), 598-700.
- Frydman, S. and Shamam I. (1989), “Pullout capacity of slab anchors in sand”, *Can. Geotech. J.*, **26**(3), 385-400.
- Ghaly, A.M. and Hanna, A.M. (1994), “Model investigation of the performance of single anchors and groups of anchors”, *Can. Geotech. J.*, **31**(2), 273-284.
- Ghaly, A., Hanna, A.M. and Hanna, M.S. (1991), “Uplift behavior of screw anchors in sand. I: Dry sand”, *J. Geotech. Engrg. Div.*, **117**(5), 773-793.
- Giffels, W.C., Graham, R.E. and Mook, J.F. (1960), “Concrete cylinder anchors”, *Electrical World*, **154**, 46-49.
- Hanna, T.H., Sparks, R. and Yilmaz, M. (1972), “Anchor behavior in sand”, *J. Soil Mech. Found. Div.*, **98**(11), 1187-1208.

- Ilamparuthi, K. and Dickin, E.A. (2001), "The influence of soil reinforcement on the uplift behavior of belled piles embedded in sand", *Geotext. Geomembr.*, **19**(1), 1-22.
- Ilamparuthi, K., Dickin, E.A. and Muthukrisnaiah, K. (2002), "Experimental investigation of the uplift behaviour of square plate anchors embedded in sand", *Can. Geotech. J.*, **39**(3), 648-664.
- Ireland, H.O. (1963), "Uplift resistance of transmission tower foundations: Discussion", *J. Power Div. ASCE*, **89**(PO1), 115-118.
- Kame, G.S., Dewaikar, D.M. and Choudhury, D. (2010), "Passive thrust on a vertical retaining wall with horizontal cohesion-less backfill", *Communicated to Soils and Rocks, Int. J. of Geotech. Geo-Env. Eng., Brazil*.
- Kame, G.S., Dewaikar, D.M. and Choudhury, D. (2012), "Pullout capacity of vertical plate anchors in cohesion-less soil", *Geomech. Eng., Int. J.*, **4**(2), 105-120.
- Kananyan, A.S. (1966), "Experimental investigation of the stability of bases of anchor foundations", *Osnovanlyya, Fundamenty i mekhanik Gruntov*, **4**(6), 387-392.
- Krishnaswamy, N.R. and Parashar, S.P. (1994), "Uplift behavior of plate anchors with geosynthetics", *Geotext. Geomembr.*, **13**(2), 67-89.
- Kumar, J. and Kouzer, K.M. (2008), "Vertical uplift capacity of horizontal anchors using upper bound limit analysis and finite elements", *Can. Geotech. J.*, **45**(5), 698-704.
- Kuzer, K.M. and Kumar, J. (2009), "Vertical uplift capacity of two interfering horizontal anchors in sand using an upper bound limit analysis", *J. Computer Geotechnic.*, **1**(36), 1084-1089.
- Liu, J., Liu, M. and Zhu, Z. (2012), "Sand deformation around an uplift plate anchor", *J. Geotech. Geoenviron. Eng.*, **138**(6), 728-737.
- Mariupolskii, L.G. (1965), "The bearing capacity of anchor foundations", *SM and FE, Osnovanlyya, Fundamenty i mekhanik Gruntov*, **3**(1), 14-18.
- Merifield, R. and Sloan, S.W. (2006), "The ultimate pullout capacity of anchors in frictional soils", *Can. Geotech. J.*, **43**(8), 852-868.
- Meyerhof, G.G. (1973), "Uplift resistance of inclined anchors and piles", *Proceedings 8th International Conference on Soil Mechanics and Foundation Engineering*, Vol. 2, Moscow, pp. 167-172.
- Meyerhof, G.G. and Adams, J.I. (1968), "The ultimate uplift capacity of foundations", *Can. Geotech. J.*, **5**(4), 225-244.
- Mors, H. (1959), "The behaviour of mast foundations subjected to tensile forces", *Bautechnik*, **36**(10), 367-378.
- Murray, E.J. and Geddes, J.D. (1987), "Uplift of anchor plates in sand", *J. Geotech. Engrg.*, **113**(3), 202-215.
- Niroumand, H. and Kassim, K.A. (2013), "Uplift response of symmetrical anchor plates in reinforced cohesionless soil", *Arabian J. Geosci.*, 1-12. DOI: 10.1007/s12517-013-1071-6
- Ovesen, N.K. (1981), "Centrifuge tests of the uplift capacity of anchors", *Proceedings of the 10th International Conference on Soil Mechanics and Foundation Engineering*, Stockholm, pp. 717-722.
- Rowe, R.K. and Davis, E.H. (1982), "The behaviour of anchor plates in clay", *Geotechnique*, **32**(1), 9-23.
- Sarac, D.Z. (1989), "Uplift capacity of shallow buried anchor slabs", *Proceedings of the 12th International Conference of Soil Mechanics and Foundation Engineering*, Rio de Janeiro, Brazil, Vol. 2, pp. 1213-1218.
- Selvadurai, A.P.S. (1989), "Enhancement of the uplift capacity of buried pipelines by the use of geogrids", *Geotech. Test. J.*, **12**(3), 211-216.
- Selvadurai, A.P.S. (1993), "Uplift behavior of strata-grid anchored pipelines embedded in granular soils", *J. Geotech. Engrg.*, **24**(1), 39-55.
- Smith, C.C. (1998), "Limit loads for an anchor/trapdoor embedded in an associated coulomb soil", *Int. J. Numer. Anal. Methods Geomech.*, **22**(11), 855-865.
- Subbarao, C., Mukhopadhyay, S. and Sinha, J. (1988), "Geotextile ties to improve uplift resistance of anchors", *Proceedings of the 1st Indian Geotextile Conference on Reinforced Soil and Geotextiles*, Bombay, India, Balkema, Rotterdam, pp. F3-F8.
- Sutherland, H.B. (1965), "Model studies for shaft raising through cohesionless soils", *Proceedings of the 6th International Conference Soil Mechanics and Foundation Engineering*, Montreal, Quebec, Canada, Vol. 2,

- pp. 410-413.
- Sutherland, H.B., Finlay, T.W. and Fadl, M.O. (1982), "Uplift capacity of embedded anchors in sand", *Proceedings of the 3rd International Conference on the Behavior of Offshore Structures*, Cambridge, MA, USA, pp. 451-463.
- Tagaya, K., Scott, R.F. and Aboshi, H. (1988), "Pull-out resistance of buried anchors in sand", *Soil. Found.*, **28**(3), 114-130.
- Trautmann, C.H. and Kulhawy, F.H. (1988), "Uplift load-displacement behavior of spread foundations", *J. Geotech. Engrg. Div.*, **114**(2), 168-184.
- Turner, E.Z. (1962), "Uplift resistance of transmission tower footings", *J. Power Div. ASCE*, **88**(PO2), 17-33.
- Vesic, A.S. (1971), "Break-out resistance of objects embedded in ocean bottom", *J. Soil Mech. Found. Div. ASCE*, **97**(9), 1183-1205.

CC